An 8-Zone Test System based on ISO New England Data: Development and Application

Dheepak Krishnamurthy, *Student Member, IEEE,* Wanning Li, *Student Member, IEEE,* and Leigh Tesfatsion, *Member, IEEE*

***Abstract*—This study develops an open-source 8-zone test system for teaching, training, and research purposes that is based on ISO New England structural attributes and data. The test system models an ISO-managed wholesale power market populated by a mix of generating companies and load-serving entities that operates through time over an 8-zone AC transmission grid. The modular extensible architecture of the test system permits a wide range of sensitivity studies to be conducted. To illustrate the capabilities of the test system, we report energy cost-savings outcomes for a comparative study of stochastic versus deterministic DAM Security Constrained Unit Commitment (SCUC) formulations under systematically varied reserve requirement levels for the deterministic formulation.**

***Index Terms*—Electricity market, 8-Zone ISO-NE Test System, SCUC, stochastic optimization**

I. Introduction

A. General Features of the 8-Zone ISO-NE Test System

THE 8-Zone ISO-NE Test System developed in this study, based on structural attributes and data from the New England Independent System Operator (ISO-NE), is an empirically-grounded open-source support tool for power market teaching, training and research. It is a relatively small-scale test system that has been designed to permit the systematic exploratory study of power market design and performance issues for ISO-NE by means of extensive fast-execution computational experimentation.[1]

Specifically, the test system models a wholesale power market operating through time over an AC transmission grid with congestion managed by locational marginal pricing (LMP). The modeled energy region is divided into eight zones, in accordance with the eight designated load zones for ISO-NE; and generation, load, and transmission line attributes are configured on the basis of current ISO-NE data.

Important Note: Latest revision – 12 January 2017. This revision corrects some garbled expressions appearing in the appendix SCUC equations in the published paper version: IEEE Transactions on Power Systems 31(1), Jan 2016, 234-246. D. Krishnamurthy and W. Li are with the Department of Electrical and Computer Engineering, Iowa State University, Ames, IA 50011 USA (e-mail: {dheepakk,wanningl}@iastate.edu). L. Tesfatsion (corresponding author) is with the Department of Economics, Iowa State University, Ames, IA 50011 USA (e-mail: tesfatsi@iastate.edu). This work has been supported in part by an ARPA-E award (DE-AR00002014) from the Department of Energy.

[1]DOE's Technology Readiness Levels [1] range from TRL 1 (initial conceptual development) to TRL 9 (commercial application). Under the DOE ARPA-E project that funded this study's research, with ISO-NE as a participating partner, the 8-Zone ISO-NE Test System was deliberately designed as a TRL 4 test system to help bridge the "valley of death" (TRLs 4-6) that must be crossed in order to bring typical university research (TRLs 1-3) into contact with typical industry research (TRLs 7-9).

The day-ahead and real-time markets modeled by this test system involve ISO-managed bid/offer-based security-constrained unit commitment (SCUC) and security-constrained economic dispatch (SCED) optimal power flow (OPF) optimizations for the determination of unit commitment, dispatch, and pricing solutions. These solutions are calculated and implemented day after day, where the system state at the beginning of each day D is determined as a function of the previous state at the beginning of day D-1 together with internal system events and external environmental events occurring during day D-1.

This dynamic state-space modeling approach permits the study of both market efficiency and system reliability over time. For example, the effects of a change in a market operating procedure on the welfare (profits and losses) of market participants, and on the stability of system operations as a whole, can be studied over the short, intermediate, and long run, taking into account the responses of market participants and system conditions to this change.

Although the 8-Zone ISO-NE Test System is configured using structural attributes and data from ISO-NE, it is implemented by means of the AMES Wholesale Power Market Test Bed [2], a Java/Python package of classes with a modular and extensible architecture. Consequently, users of the test system can easily modify its features to match the operations of other wholesale power markets, or to model and study proposed market design elements that have not yet been implemented. For example, the test system's Graphical User Interface (GUI) permits users to vary the generation mix for their own purposes by introducing generation units with distinct names, locations, fuel types, capacities, start-up costs, no-load costs, dispatch cost coefficients, and ramping capabilities.

B. Comparison with Previously Developed Test Systems

The 8-Zone ISO-NE Test System differs in purpose, availability, and scale from previously developed test systems for power system analysis.

Some researchers in collaboration with industry partners have been able to make use of ISO/RTO-scale systems; see, for example, [3]. However, these systems are not open source and are not easy to access for most researchers. Moreover, the systems are so large and complex that it is difficult to use them for intensive sensitivity studies.

Other researchers have developed publicly available test systems; but, to date, these systems have largely been designed to facilitate the study of system stability at relatively small time

scales rather than the study of market performance over successive days. Examples include the IEEE reliability test systems stored at the University of Washington archive ([4],[5]) as well as more recently developed test systems such as [6] and [7]. For example, in [7] a power flow study is conducted for a 68-bus system to determine initial steady-state values, and state-space matrices and eigenvalues are then determined for the linearized system at this initial point in order to enable a study of local system stability.

The traditional IEEE benchmark-system focus on power flow problems for local stability analysis has been extended in more recent test systems and software packages to permit a consideration of OPF solutions based on the bids and offers of market participants. This development reflects the increasing use of OPF optimizations in centrally-managed wholesale power markets.

For example, MATPOWER [8] is a package of Matlab M-files designed for solving both power flow and OPF problems. Nevertheless, the focus of MATPOWER is still on stability issues arising at relatively small time scales. Moreover, although top-level MATPOWER code is now being distributed under a GNU General Public License (GPL), MATPOWER is based on Matlab for which core aspects are proprietary; hence, exceptions are included in the GPL to ensure proprietary Matlab code is protected.

In recent years a number of researchers have attempted to redress the relative lack of publicly available market-oriented test systems. For example, variants of a 5-bus test system originally developed in 2002 by John Lally [9, Section 6] for the study of the financial transmission rights market in ISO-NE are now being used for more general market training by ISO-NE, PJM, and other ISO/RTO-managed U.S. energy regions.

As detailed in Sun and Tesfatsion [10] and Li and Tesfatsion [11], the Lally 5-bus test system has been developed into a more fully articulated 5-Bus Test Case included (along with a 2-Bus Test Case and a 30-Bus Test Case) in the open-source release of the AMES Wholesale Power Market Test Bed [2]. In addition, Li and Bo [12] have suggested various ways to improve a version of the Lally 5-bus test system in use by PJM, such as the introduction of differentiated loads across the three load buses for increased clarity. Li and Bo also discuss a number of modifications proposed by themselves and others for the IEEE 30-bus reliability test system that would increase its usefulness for market study purposes.

In contrast to the 8-Zone ISO-NE Test System, however, the specification of structural attributes and parameter values for these previously developed small-scale market-oriented test systems are largely arbitrary, for illustrative purposes only. No attempt has been made to base these specifications on the empirical conditions of an actual energy region.

The 8-Zone ISO-NE Test System also differs in purpose from larger-scale market-oriented test systems, such as the FERC test system [13] and the WECC test system [14]. These test systems have been designed for commercial-grade application, not for exploratory fast-execution simulation studies. The FERC test system provides a large-scale PJM-based data set and unit commitment (UC) formulation to facilitate the comparative study of alternative DAM and residual UC solvers. The 240-bus WECC test system provides a realistic large-scale test system for the California Independent System Operator (CAISO) and the Western Electricity Coordination Council (WECC) for the purpose of studying possible improvements to existing market features.

C. Motivation for the Illustrative Application

The recent rapid growth of variable generation, resulting in increased supply uncertainty, has encouraged efforts to develop improved stochastic security-constrained unit commitment (SCUC) optimization tools. See, for example, Morales et al. [15], Papavasiliou et al. [16], and Vrakopoulou et al. [17].

To illustrate the capabilities of the 8-Zone ISO-NE Test System, we report on its use for a comparative study of stochastic versus deterministic DAM SCUC formulations under varied reserve requirement levels for the deterministic formulation.[2] In contrast to previous comparative SCUC studies (e.g., [16]), performance is measured in terms of energy cost saving taking into account both day-ahead unit commitment costs and real-time dispatch costs.

Also, a detailed analysis is undertaken to understand the reasons for observed performance differences. Specifically, the reported results reveal the critical roles played by scenario specification bias, load dispersion, generation mix, and reserve requirements in determining the extent to which a switch from a deterministic to a stochastic DAM SCUC formulation results in energy cost savings.

D. Study Organization

The remainder of this study is organized as follows. Section II discusses the computational platform (AMES) used to implement the 8-Zone ISO-NE Test System. Section III describes the basic components of the test system. An illustrative application of this test system, a comparison of stochastic vs. deterministic DAM SCUC formulations, is discussed in Section IV, and key findings from this illustrative application are reported in Section V. Concluding remarks are given in VI.

Finally, a detailed mathematical presentation of the stochastic DAM SCUC formulation for our illustrative application is provided in an appendix, together with a nomenclature table. Complete Java/Python code files and data files for the 8-Zone ISO-NE Test System are provided at [18].

II. Implementation via the AMES Test Bed

In a 2003 report [19] the U.S. Federal Energy Regulatory Commission (FERC) proposed the adoption of a market design for improved wholesale power system operations. This design has since been implemented in seven U.S. energy regions

[2]As will be clarified in Section IV, it is commonly assumed for stochastic SCUC optimizations that the set of scenarios specified for possible future load realizations covers all possible uncertainties, and that power-balance constraints are scenario-conditioned. Consequently, reserve-requirement constraints are not considered. In practice, it might of course be prudent to continue to impose reserve-requirement constraints to insure against the possibility that the specified scenario set does not in fact provide complete coverage of uncertainties.

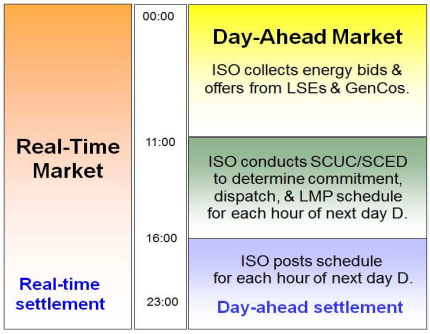

Fig. 1. Two-settlement market design: ISO activities on a typical day D-1

encompassing over 60% of U.S. generation capacity. The core feature of this design is a two-settlement system, centrally managed by an independent system operator (ISO) or regional transmission organization (RTO).

As depicted in Fig. 1, this two-settlement system consists of a daily day-ahead market (DAM) for the commitment and scheduling of generation for next-day operations and a daily 24-hour real-time market (RTM) functioning as a balancing mechanism to handle any residual load-balancing needs. In both markets, transmission congestion is managed by locational marginal pricing (LMP).

AMES (Agent-based Modeling of Electricity Systems) [2] is an agent-based Java/Python computational platform permitting the systematic study of dynamic wholesale power systems structured in accordance with FERC's two-settlement market design. The 8-Zone ISO-NE Test System developed in this study is implemented by means of AMES(V4.0).

As depicted in Fig. 2, AMES(V4.0) models an ISO-managed wholesale power market operating during time-periods $k = 1, 2, \ldots$, over an AC transmission grid. Participants in this market include Generation Companies (GenCos) as well as Load-Serving Entities (LSEs) servicing the energy needs of retail customers. The GenCos can include generators (e.g., thermal) with dispatchable power as well as generators (e.g., solar, wind) with non-dispatchable power treated as negative load.

The dispatchable GenCos submit supply offers into the DAM and the RTM consisting of fixed and/or price-responsive portions. The LSEs submit demand bids into the DAM consisting of fixed and/or price-responsive portions. AMES(V4.0) includes a learning module that permits GenCos and/or LSEs to be modeled as learning agents capable of changing their offer/bid methods over time on the basis of past experiences.

In the DAM, the ISO conducts bid/offer-based SCUC and bid/offer-based SCED optimizations to determine the commitment and scheduled dispatch of generation to meet forecasted next-day loads, as determined from LSE demand bids. In the RTM, the ISO conducts an offer-based SCED optimization to resolve imbalances between DAM-scheduled generation and ISO forecasted real-time loads. A cost for curtailed load is included in the SCUC/SCED objective functions as a summation of power-balance slack terms multiplied by a user-specified penalty weight.

Dispatchable GenCos in AMES(V4.0) can incur both UC and dispatch costs, where the UC costs take the form of start-up, no-load, and shut-down costs. The performance metric considered in later sections of this study is cost saving, where cost consists of both UC costs and dispatch costs measured in terms of energy usage.[3] Consequently, it is important to understand the precise distinctions among these various types of costs.

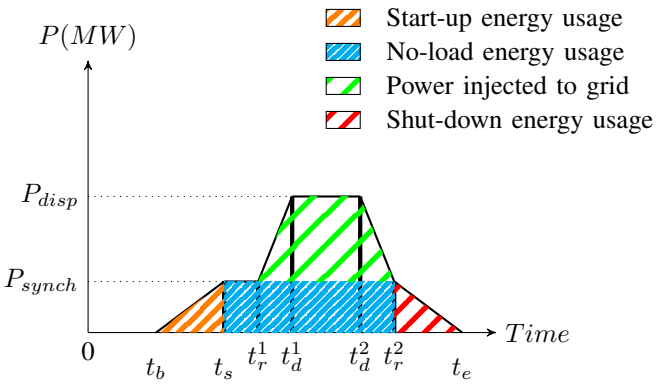

Fig. 3. Energy usage over time for a generation unit

Figure 3 illustrates the various ways that a generator can use energy as a result of commitment and dispatch, and hence incur UC and dispatch costs. In Fig. 3, a dispatchable generator g in a shut-down condition at time 0 is scheduled to inject power into the grid at level $P = [P_{\text{disp}} - P_{\text{synch}}]$ during time interval $[t_d^1, t_d^2]$. During the time interval $[t_b, t_s]$, g ramps up to the power level P_{synch} at which it is spinning at synchronous speed, ready to inject power into the grid. During the time interval $[t_s, t_r^1]$, g remains in a synchronized state with no injection of power into the grid. During time interval $[t_r^1, t_d^1]$, g ramps up to reach the power level P_{disp}; and g maintains this power level over the time interval $[t_d^1, t_d^2]$. At time t_d^2 generator g initiates a ramp-down process. During the initial ramp-down stage $[t_d^2, t_r^2]$, g is still injecting power into the grid. At time t_r^2, g reaches the power level P_{synch} at which it is synchronized to the grid but not injecting power into the grid. Generator g then continues to ramp down until it reaches a shut-down state at time t_e.

The costs of the energy used by g over the time interval $[t_b, t_s]$ to attain a synchronized state, starting from a shut-down state, are called *start-up costs*. The costs of the energy used by g to remain synchronized during the time interval $[t_s, t_r^2]$ are called *no-load costs*. The costs of the energy injected by g into the grid during the scheduled dispatch interval $[t_d^1, t_d^2]$ are called *dispatch costs*.[4] Finally, the costs of the energy used by g over the time interval $[t_r^2, t_e]$ to attain a shut-down state, starting from a synchronized state, are called *shut-down costs*.

AMES(V4.0) calculates dispatch and start-up/shut-down costs by dispatch and start-up/shut-down energy usage, as

[3]UC costs can also include non-energy related costs, such as the wear and tear on machinery from the start-up, shut-down, and/or synchronized running of generation units. In AMES(V4.0) only energy costs are considered.

[4]In current U.S. DAM operations, generators are typically not compensated for the energy they expend in ramping from a syncronized state to a scheduled dispatch level that is about to start or back to a synchronized state from a scheduled dispatch level that has just concluded.

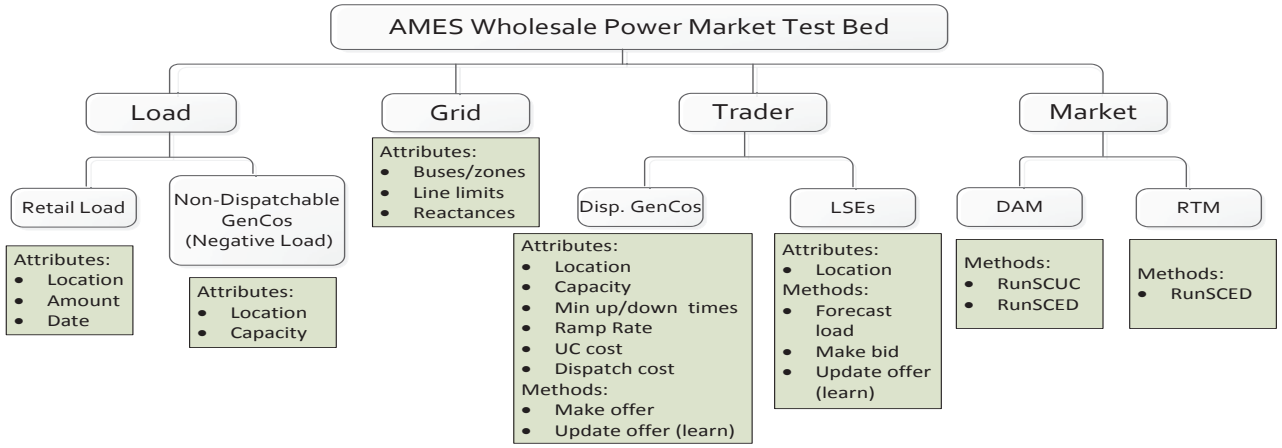

Fig. 2. Key components of AMES(V4.0)

depicted in Fig. 3. However, no-load costs are calculated only for the duration of time during which a generator is dispatched. That is, the presumption is that a committed generator can time its synchronization point to coincide with the start of its dispatch period so that no-load energy usage as depicted by the energy block t_s-t_r^1-P_{synch} in Fig. 3 does not arise.

III. The 8-Zone ISO-NE Test System

This section discusses our construction and benchmark configuration of the 8-Zone ISO-NE Test System based on ISO-NE structural attributes and data.[5] Detailed code and benchmark data configuration files for the test system can be obtained at the repository site [18]. A user can either keep our benchmark settings or change them to user-specified values via the test system's graphical user interface (GUI).

A. Transmission Grid

ISO-NE is part of the Northeast Power Coordinating Council (NPCC) reliability region. The states covered by ISO-NE are Connecticut, Maine, Massachusetts, New Hampshire, Rhode Island and Vermont. The ISO-NE energy region is divided into eight load zones: namely, Connecticut (CT), Maine (ME), New Hampshire (NH), Rhode Island (RI), Vermont (VT), Northeastern Massachusetts/Boston (NEMA/BOST), Southeastern Massachusetts (SEMA) and Western/Central Massachusetts (WCMA) [20].

To reflect this configuration, our 8-Zone ISO-NE Test System consists of eight zones connected by an AC transmission grid consisting of twelve transmission lines; see Fig. 4. Flows with neighboring energy regions are not considered. Since transmission projects placed in service in ISO-NE over the past decade have substantially reduced congestion, the benchmark capacity (power limit) of each line in the 12-line test-system grid is set at a relatively high level.

[5]Some data were directly supplied to us by ISO-NE, a participating partner in the ARPA-E project that supported our research. However, these data were incomplete in some regards for our market analysis purposes. As clarified below, the needed missing data were obtained from other reliable sources.

The resistance and reactance benchmark values for the 12-line test-system grid are set based on physical considerations. The key factors that determine these values include the length of each line, conductor type, conductor bundling and transposition, and temperature. Each line is assumed to be a single-circuit 345kV AC line with a 6-conductor bundle per phase, using conductor type Dove (556 kcmil). The bundles have $2.5'$ diameter and the phases are separated by $45'$. The temperature is assumed to be constant at 25 degrees Celsius. Given these physical attributes, resistance and reactance values (per unit of length) are derived from ACSR cable parameter tables for overhead transmission lines: namely, Table A8.1 in [21] and Tables 3.3.1-3.3.13 in [22].

The length of each line in our 12-line test-system grid is measured by the distance between the two ISO-NE zones that it connects, where each zone is represented as a point located at a central city within the zone. The benchmark resistance and reactance values for each line are then obtained by multiplying the resistance and reactance values (per unit of length) by the line length; see Table I. In the last column of Table I, reactance (ohms) is converted into per unit (pu) using 345kV as the base voltage value and 100MVA as the base volt-ampere value.

TABLE I
Resistance and Reactance Benchmark Values for the 8-Zone ISO-NE Test System

Line	From Zone	To Zone	Distance (miles)	Resistance (ohms)	Reactance (ohms)	Reactance (per unit)
1	ME	NH	115.00	19.09	54.05	0.05
2	VT	NH	100.00	16.60	47.00	0.04
3	VT	WCMA	150.00	24.90	70.50	0.06
4	WCMA	NH	86.00	14.28	40.42	0.03
5	NEMA/BOST	WCMA	80.00	13.28	37.60	0.03
6	NEMA/BOST	NH	63.00	10.46	29.61	0.02
7	NEMA/BOST	SEMA	30.00	4.98	14.10	0.01
8	WCMA	CT	30.00	4.98	14.10	0.01
9	WCMA	RI	65.00	10.79	30.55	0.03
10	NEMA/BOST	RI	40.00	6.64	18.80	0.02
11	CT	RI	64.00	10.62	30.08	0.03
12	SEMA	RI	20.00	3.32	9.40	0.01

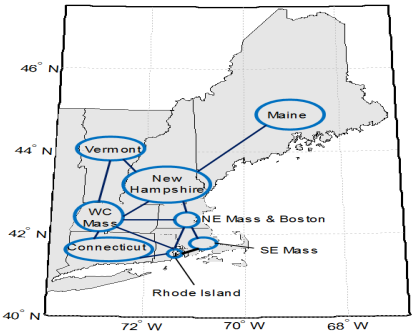

Fig. 4. Transmission grid for the 8-Zone ISO-NE Test System

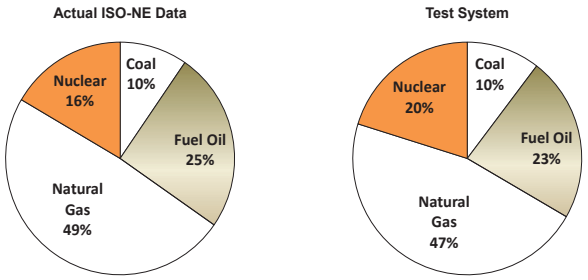

Fig. 5. Comparison of ISO-NE and 8-Zone ISO-NE Test System thermal generation capacity proportions by fuel type

B. Generator Attributes

As detailed in [23], the generation mix for ISO-NE currently consists of 436 generation units with a total installed capacity of 32,000MW. Roughly 88% of this capacity is provided by 151 thermal generation units. The remaining 12% is provided by generation units consisting of traditional hydro (4%), pumped hydroelectric storage (5%), and other renewables (3%). The latter category includes 73 wind farms (2.5%), generally small in size.

To obtain a benchmark generation mix for our 8-Zone ISO-NE Test System, this actual ISO-NE generation mix was reduced in size as follows. First, all non-thermal generation units were removed. This was done to avoid having to undertake relatively complicated special modeling for only a small portion of total installed generation capacity.[6]

Second, 76 of the remaining 151 thermal generation units were selected for inclusion in the benchmark generation mix, each treated as an independent generator. These 76 generators have a combined installed generation capacity of 23,100MW and account for 72% of the actual ISO-NE capacity (32,000MW). As indicated in Fig. 5, in implementing this selection, care was taken to ensure that the overall proportions of thermal generation (by fuel type) for the test system roughly match the overall proportions of thermal generation (by fuel type) in ISO-NE. In addition, care was taken to ensure that the proportions of thermal generation (by fuel type) specified for each of the eight zones in the test system roughly match the actual proportions of thermal generation (by fuel type) in each of the eight corresponding ISO-NE load zones.

The 76 benchmark thermal generators for the 8-Zone ISO-NE Test System incur both UC costs and dispatch costs, where the UC costs include start-up, no-load, and shut-down costs. Additional generator attributes in need of specification include ramp rates and minimum up/down times.

The MBtu per start for a generator is classified as hot or cold, depending on the time that the generator has been offline. These hot/cold values can differ, and they depend on the generator's fuel type and capacity. The hot/cold MBtu per start for a generator multiplied by the cost per MBtu for that generator's fuel type gives the generator's hot/cold start-up costs. Similarly, the MBtu per stop for a generator multiplied by the cost per MBtu for that generator's fuel type gives the generator's shut-down costs. Data on hot/cold MBtu/start and MBtu/stop for different fuel types and capacities were obtained from the provided ISO-NE data. The costs per MBtu for generators with different fuel types were obtained from the U.S. Energy Information Administration (EIA) [24].

The no-load cost for each of the benchmark thermal generators by fuel type and capacity was derived from the detailed data provided in [25] for ISO-NE energy offer data. A summary indication of these no-load costs by fuel type and capacity range is given in Table II.

TABLE II
NO-LOAD COSTS BY FUEL TYPE AND CAPACITY.

Fuel type	Capacity (MW)	No-load cost ($/hr)
Coal	0 – 75	236 – 238
Coal	75 – 150	238 – 745
Coal	150 – 350	745 – 1213
Coal	> 350	1213 – 3043
Fuel Oil	0 – 80	0 – 1500
Fuel Oil	80 – 200	1500 – 2000
Fuel Oil	200 – 400	2000 – 3500
Fuel Oil	400 – 600	3500 – 10379
Natural Gas	0 – 400	0 – 600
Natural Gas	400 – 600	600 – 3859
Nuclear	—-	1000 – 1500

The total dispatch cost function ($/h) for each benchmark generator g in each hour k is assumed to take the following form:

$$C_{P,g} = a_g p_g + b_g [p_g]^2 \quad (1)$$

where p_g (MW) denotes g's power output. Benchmark settings for the cost coefficients a_g and b_g in (1) were derived from ISO-NE generation block-offer schedule data differentiated by

[6]The modeling of hydro units is relatively complicated, requiring water resource planning and optimization techniques involving considerations of water supply, reservoir management, and flood control. This modeling is further complicated by the need to consider seasonal and cyclic variability of stochastic quantities such as reservoir inflows. Furthermore, these types of generation units often resort to self-scheduling of their generation offers in the DAM, hence there is only limited information on their offer methods. Similarly, the inclusion of wind generation would require a careful modeling of the special treatment of wind generation in the ISO-NE, including the extent to which the ISO-NE permits wind generation to be offered into the DAM, the extent to which the ISO-NE is able to use wind spillage as reg down, and the manner in which sudden strong ramp events caused by wind penetration are handled. However, as noted in Section II, our test system is implemented by means of the modular and extensible AMES(V4.0) test bed. This should facilitate the inclusion of hydro, wind, and other renewable generation sources in future extensions of our test system.

fuel type [25]. A summary indication of these benchmark cost-coefficient settings by fuel type is given in Table III.

TABLE III
DISPATCH COST COEFFICIENTS BY FUEL TYPE.

Fuel type	a ($/MWh)	b ($/MW^{2}h)
Coal (BIT)	18.28	0.000116
Coal (SUB)	19.98	0.001667
Fuel Oil	150 – 233	0.0059 – 0.0342
Natural Gas	23.13 – 57.03	0.002 – 0.008
Nuclear	5-11	0.00015 – 0.00023

A generator's ramp rate (MW/min) is the amount by which the generator can ramp its power output up or down in one minute. Ramp rates by fuel type, provided in [26], are displayed in Table IV. These ramp rates were used to configure the ramp rates for the benchmark generators. Finally, minimum up/down times for the benchmark generators were fully specified on the basis of provided ISO-NE data.

TABLE IV
RAMP RATES BY FUEL TYPE.

Fuel Type	Ramp Rate MW/min
Coal	2.0
Fuel Oil	2.0
Natural Gas	6.7
Nuclear	2.0

Complete attribute specifications for each of the 76 benchmark generators for the 8-Zone ISO-NE Test System are provided at the repository site [18]. As indicated above, these specifications include zone location, fuel type, capacity, start-up costs, no-load costs, shut-down costs, dispatch cost coefficients, ramp rates, and minimum up/down times.

C. LSE Attributes

The 8-Zone ISO-NE Test System has eight zones z, each serviced by a single aggregate load-serving entity LSE_z. Specifically, LSE_z submits a demand bid into the DAM on each day D-1 that takes the form of a forecasted 24-hour zone-z load profile for day D.[7]

As will be clarified in Section IV-C, the load scenarios used in the illustrative application of the 8-Zone ISO-NE Test System are based on actual ISO-NE load data; and LSE load forecasts take the form of load expectations (probability-weighted averages) calculated on the basis of these load scenarios.

D. Reserve Requirements

The 8-Zone ISO-NE Test System permits the inclusion of user-specified zonal and system-wide reserve requirements in the day-ahead and/or real-time SCUC/SCED optimizations. Reserve in the 8-Zone ISO-NE Test System consists of the unencumbered (non-dispatched) capacity of the DAM-committed generators.[8] System-wide reserve consists of the unencumbered capacity of all committed generators, regardless of their location. Zonal reserve for a particular zone z consists of the unencumbered capacity of all committed generators located in zone z.

IV. ILLUSTRATIVE APPLICATION: OVERVIEW

A. Purpose and General Scope

To illustrate the capabilities of the 8-Zone ISO-NE Test System, we have used the test system to conduct a comparative study of stochastic versus deterministic DAM SCUC formulations. For simplicity of exposition, this illustrative application assumes: (i) the only source of uncertainty at the time of the DAM is possible next-day load-profile realizations; (ii) the power limits for the 12-line test-system grid are set high enough to ensure that no transmission congestion occurs; and (iii) the deterministic DAM SCUC formulation includes a system-wide reserve-requirement constraint but no zonal reserve constraints.

Attention is focused on the degree to which a switch from a deterministic to a stochastic DAM SCUC formulation would result in cost saving under variously specified reserve-requirement levels for the deterministic formulation. For the stochastic formulation, the ISO conditions its optimization on a set $\mathcal{S}$ of scenarios for possible future load realizations, together with associated scenario probabilities. For the deterministic formulation, the ISO conditions its optimization on an *expected* future load realization calculated on the basis of these same scenarios and probabilities.[9]

To illustrate how our test system can be used to test the robustness of alternative DAM SCUC formulations against errors in the ISO's modeling of uncertain loads, we assume the ISO's anticipated load-scenario set $\mathcal{S}$ contains only five load scenarios when, in actuality, ten load scenarios are possible.

B. Stochastic vs. Deterministic DAM SCUC Formulations

Our stochastic DAM SCUC formulation is based on the well-known deterministic SCUC formulation developed by Carrion and Arroyo [27]. We extended the Carrion/Arroyo formulation to a two-stage stochastic DAM SCUC formulation. The complete structural form of this stochastic DAM SCUC formulation is provided in an appendix, together with a nomenclature table. Here we give a summary outline of this formulation.

[7]To date, the vast majority of loads in ISO-NE are not directly responsive to wholesale prices, and the current construction of the 8-Zone ISO-NE Test System reflects this reality. However, AMES(V4.0) permits LSE demand bids to be price responsive, hence the 8-Zone ISO-NE Test System could easily permit this as well.

[8]In actual ISO-NE operations, the commitment of generators with low UC costs and high dispatch costs can be delayed until later residual unit commitment processes, called Reserve Adequacy Analysis (RAA) processes in ISO-NE, if these generators are quick-start fast-ramp units. Currently our test system only includes a DAM SCUC/SCED and an RTM SCED; it does not include RAA processes. Consequently, we include all generators in the DAM to approximate the total commitment that would occur with both a DAM and a subsequent RAA process.

[9]As will be clarified below, the expectation for each zone-conditioned scenario in the ISO's anticipated load-scenario set $\mathcal{S}$ coincides, by construction, with the corresponding zonal load-profile forecast implied by DAM LSE demand bids. In actual ISO-NE deterministic DAM SCUC operations, the ISO is required to use LSE demand bids as its forecasted next-day loads.

The objective of the ISO in our stochastic DAM SCUC formulation is to minimize expected total energy cost subject to system and UC constraints, where expectations are taken with respect to a set $\mathcal{S}$ of scenarios for possible future loads. As will be explained in Section IV-C, the scenarios in $\mathcal{S}$ are mean-zero perturbations of LSE demand bids.

Expected total energy cost is then the summation of *first-stage costs* (i.e., DAM UC costs) plus the expected level of *second-stage costs* (i.e., real-time dispatch costs plus penalty costs imposed for any real-time load curtailment). Using nomenclature defined in the appendix, expected total energy cost in analytical form is given by

$$\sum_{k\in K}\sum_{g\in\mathcal{G}}[C_{U,g}(k)+C_{N,g}(k)+C_{D,g}(k)] + \sum_{s\in S}\pi^s\sum_{k\in K}\sum_{g\in\mathcal{G}}C^s_{P,g}(k)+\Lambda\sum_{s\in S}\pi^s\sum_{z\in\mathcal{Z}}\sum_{k\in K}\gamma^s(z,k) \quad (2)$$

The decision variables for our stochastic DAM SCUC formulation are classified as follows:

- First-stage decision variables: Generator on/off commitment indicator variables, not scenario-conditioned
- Second-stage decision variables: Scenario-conditioned generator dispatch and voltage angle levels

The key types of system and UC constraints are as follows:

- Scenario-conditioned power balance constraints (by zone)
- Scenario-conditioned generation capacity constraints
- Scenario-conditioned transmission line constraints
- Scenario-conditioned ramp constraints
- Start-up/shut-down constraints
- Minimum up/down time constraints

Our deterministic DAM SCUC formulation is derived from our stochastic DAM SCUC formulation as follows. We first consider the reduced form of our stochastic DAM SCUC formulation obtained by considering only one load scenario $\bar{s}$, calculated as the expectation (probability-weighted average) of the load scenarios in the scenario set $\mathcal{S}$ for the stochastic case. The objective function for this deterministic DAM SCUC formulation thus takes the following form:

$$\sum_{k\in K}\sum_{g\in\mathcal{G}}\left[C_{U,g}(k)+C_{N,g}(k)+C_{D,g}(k)+C^{\bar{s}}_{P,g}(k)\right] + \Lambda\sum_{z\in\mathcal{Z}}\sum_{k\in K}\gamma^{\bar{s}}(z,k) \quad (3)$$

We next augment the constraints for this reduced single-scenario DAM SCUC formulation with system-wide reserve-requirement (RR) constraints of the form

$$\sum_{g\in\mathcal{G}}\overline{p}^{\bar{s}}_g(k)\geq\sum_{z\in\mathcal{Z}}L^{\bar{s}}(z,k)+RR(k) \quad (4)$$

for each hour $k \in K$, where: $\overline{p}^{\bar{s}}_g(k)$ (MW) denotes the maximum available power output of generator g in hour k, given scenario $\bar{s}$; $L^{\bar{s}}(z,k)$ (MW) denotes the ISO's forecasted load for zone z in hour k, given scenario $\bar{s}$; and $RR(k)$ (MW) denotes the system-wide reserve requirement for hour k.

C. Construction of Load Scenarios and LSE Demand Bids

The load scenarios for our illustrative application are two-day scenarios based on scaled[10] ISO-NE March hourly load data for 2004-2006, separately reported for each of ISO-NE's eight load zones.[11]

Using these data, we first generated 90 two-day hourly load scenarios, where each load scenario consisted of eight zone-conditional components. Each of these 90 scenarios was assigned an equal probability of 1/90.

We next used a well-known scenario reduction method [28] based on similarity clustering to reduce these original 90 load scenarios to a smaller collection $\mathcal{S}$ containing five load scenarios of the form $s = (s(z_1),\ldots,s(z_8))$, where s_z denotes a two-day hourly load scenario for zone z. Each $s \in \mathcal{S}$ was then assigned a probability π^s equal to the sum of the probabilities for the original load scenarios lying in its cluster.

The elements $s \in \mathcal{S}$ are assumed to be the load scenarios that the ISO anticipates could be realized for zones $z_1,\ldots,z_8$ over days D and D+1 from the vantage point of the current DAM on day D-1. For each zone z, the demand bids submitted by LSE_z into the DAM on days D-1 and D for its retail zone-z customers on days D and D+1 are constructed to coincide with the expectation (probability-weighted average) of the elements $\{s(z) \mid s \in \mathcal{S}\}$. This construction can be given the following as-if interpretation: The ISO treats DAM LSE demand bids as unbiased forecasts for future loads and specifies possible future load scenarios as mean-zero perturbations about these unbiased forecasts.

In reality, ISOs cannot specify scenario sets that correctly and completely represent all possible future load realizations. Consequently, it is important to study how biases in an ISO's load anticipations could affect the cost performance of deterministic and stochastic DAM SCUC formulations, both individually and in comparison with each other.

A careful study of this robustness issue is beyond the scope of the current study. However, we use our illustrative application to demonstrate how the 8-Zone ISO-NE Test System could be used to implement such a study.

Specifically, we again apply the scenario reduction method [28] to the original 90 two-day hourly load scenarios, except this time we reduce these scenarios to a set $\mathcal{S}^T$ of ten load scenarios of the form $s = (s(z_1),\ldots,s(z_8))$ with associated probabilities. We then simulate "true" loads as realizations from the load-scenario set $\mathcal{S}^T$ rather than from the ISO's anticipated load-scenario set $\mathcal{S}$. Hereafter $\mathcal{S}^T$ is referred to as the *simulated-true load-scenario set*.

The manner in which the ISO's anticipated load-scenario set $\mathcal{S}$ is a biased representation of the simulated-true load-scenario set $\mathcal{S}^T$ is depicted in Fig.6, where the two sets are

[10] As detailed in Section III-B, the benchmark generation mix for our 8-Zone ISO-NE Test System is a scaled-down representation of the actual ISO-NE generation mix that captures 72% of actual ISO-NE total installed generation capacity. For consistency, we scale the load data for our illustrative application to 72% of actual ISO-NE loads.

[11] As detailed in SectionIV-D, our illustrative application uses two-day load scenarios to conduct two-day simulations. However, expected cost saving is only reported for the second day since first-day results can be distorted by initial conditions. Additional important but technical implementation details are discussed at the test system code and data repository site [18].

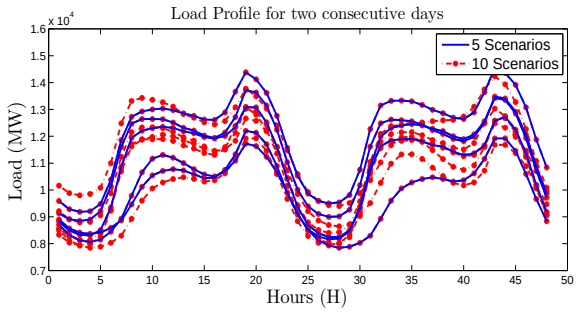

Fig. 6. Bias in the ISO's load-scenario specifications for the illustrative application, The five scenarios in the ISO's anticipated load-scenario set $\mathcal{S}$ appear as thick solid blue lines, whereas the ten scenarios in the simulated-true load-scenario set $\mathcal{S}^T$ appear as dash-dot red lines.

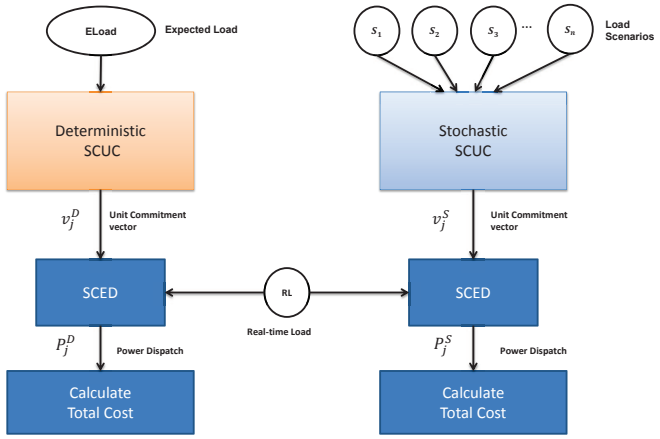

Fig. 7. Sensitivity testing procedure

superimposed.

D. Sensitivity Design

The key treatment factor highlighted in our illustrative application is the system-wide RR level set for the deterministic SCUC formulation. The range of tested RR levels is from 0MW to 8,500MW, measured in power terms, or from 0% to 61% of peak load for the tested month of March.

The performance metric for our illustrative application is (second-day) expected cost saving, calculated as the (second-day) percentage difference in expected total energy cost when the ISO switches from a deterministic to a stochastic DAM SCUC formulation. As detailed in Section IV-B, total energy cost is a summation of start-up, no-load, shut-down, dispatch, and load curtailment costs. The no-load, start-up, and shut-down costs are UC costs that arise from DAM SCUC solutions, whereas the dispatch and load curtailment costs are real-time costs that arise from RTM SCED solutions; see Fig. 7.

For each tested RR level, (second-day) expected cost saving is calculated as follows. First, select a load scenario sj from among the ten load scenarios in $\mathcal{S}^T$ to be the simulated-true load for the next two days. Second, calculate the total energy cost that would be realized over each of the the next two days, given RR and sj, assuming the ISO uses the stochastic DAM SCUC formulation conditional on its anticipated load-scenario set $\mathcal{S}$. Third, calculate the total energy cost that would be realized over each of the next two days, given RR and sj, assuming the ISO uses the deterministic DAM SCUC formulation conditional on the expected load scenario $\bar{s}$ constructed from his anticipated load-scenario set $\mathcal{S}$.

Fourth, letting $\text{TC}_{RR,sj}(\text{Det})$ and $\text{TC}_{sj}(\text{Sto})$ denote the total energy cost resulting on the second day from the implementation of the deterministic and stochastic DAM SCUC formulations, conditional on RR and sj, calculate the (second-day) *Cost Saving* that would result from a switch from a deterministic to a stochastic DAM SCUC, given RR and sj, as follows:

$$\text{CS}_{RR,sj} = \frac{\text{TC}_{RR,sj}(\text{Det}) - \text{TC}_{sj}(\text{Sto})}{\text{TC}_{RR,sj}(\text{Det})} \times 100\% \qquad (5)$$

Fifth, multiply $\text{CS}_{RR,sj}$ by the probability π^{sj} assigned to the occurrence of sj. Finally, repeat these same steps for each of the ten load scenarios $s1, \ldots, s10$ in $\mathcal{S}^T$, and calculate the (second-day) *expected cost saving*, given RR, as

$$\text{Exp. CS}_{RR} = \sum_{j=1}^{10} \pi^{sj} \text{CS}_{RR,sj} \qquad (6)$$

E. Software Implementation

All simulations for our illustrative application were implemented by running the AMES(V4.0) test bed [2] on an Intel(R) Core(TM) 2 Duo CPU E8400 @ 3Ghz machine. AMES(V4.0) uses 64-bit versions of Java (v1.8.0_25), Coopr (v3.4.7842), Python (v2.7.8), MatLab(v2014a) and CPLEX Studio (v12.51). Two threads were used to solve the unit commitment optimization problem.

V. Key Findings for the Illustrative Application

This section reports results for the illustrative application described in Section IV. A key finding is that the expected cost saving (6) resulting from a switch from a deterministic to a stochastic DAM SCUC formulation displays a U-shaped variation as the reserve requirement RR for the deterministic DAM SCUC formulation is successively increased.

Specifically, as shown in the seventh column of Table V and depicted in Fig. 8, Exp. CS_{RR} initially remains relatively flat as the reserve requirement RR is increased from 0% to 18% of peak load. As RR continues to increase, however, Exp. CS_{RR} declines until RR reaches the 25% "sweet spot" for the deterministic DAM SCUC formulation. At this sweet spot, Exp. CS_{RR} turns negative, implying that deterministic SCUC actually outperforms stochastic SCUC in terms of expected total energy costs. However, as RR continues to increase, Exp. CS_{RR} again turns positive and subsequently exhibits a dramatic increase.

In interpreting these results, it is important to consider the standard deviations for expected cost saving reported in the final column of Table V. These standard deviations indicate that the two DAM SCUC formulations do not actually result in *statistically* meaningful differences in expected total energy costs until the RR level for deterministic SCUC exceeds 36%.

TABLE V
COST SAVING (%) BY TYPE OF COST

RR (MW)	RR (% peak load)	Exp. $CS_{StartUp}$ ($)	Exp. $CS_{ShutDown}$ ($)	Exp. CS_{NoLoad} ($)	Exp. $CS_{Dispatch}$ ($)	Exp. CS_{RR} (%)	Std. CS_{RR} (%)
0	0	-52895.04	-957.90	-52228.42	670739.57	2.70	5.61
500	4	-52895.04	-957.90	-56364.85	672817.21	2.69	5.59
1000	7	-52895.04	-957.90	-56365.13	665961.40	2.64	5.58
1500	11	-52674.25	-960.00	-56367.58	651982.74	2.57	5.42
2000	14	-52895.04	-957.90	-56367.08	646205.25	2.53	5.39
2500	18	-51622.29	-932.43	-55116.10	609888.50	2.33	5.23
3000	21	-33395.04	-594.57	-41302.85	314175.47	1.21	3.72
3500	25	-39110.68	-708.87	-24764.81	84770.44	-0.30	1.16
4000	29	-17683.82	-353.66	1376.09	9797.53	-0.15	0.32
4500	32	-17651.50	-253.02	36212.88	-6072.44	0.21	0.63
5000	36	-12901.50	-158.02	66728.67	-36865.12	0.31	0.63
5500	39	2642.13	32.84	137292.27	-108595.63	0.63	0.55
6000	43	97217.88	1952.85	338930.90	-214583.16	4.22	2.08
6500	47	178901.50	3429.35	556779.82	-367302.19	6.95	2.21
7000	50	178299.17	3035.86	788327.57	-589487.46	6.84	3.50
7500	54	308679.87	1916.91	1088101.44	-743824.36	11.38	4.30
8000	57	411134.36	3921.26	1477314.68	-710729.52	18.37	6.92
8500	61	502400.47	7895.72	2127312.97	-968051.58	24.13	7.74

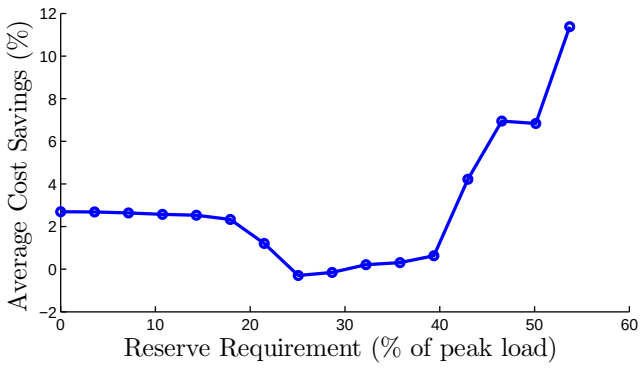

Fig. 8. Expected cost saving (%) as the reserve requirement (RR) for deterministic DAM SCUC increases from 0% to 54% of peak load for the tested month of March

Columns three through six in Table V report the sources of the expected cost saving in column seven, broken out by type of cost (start-up, shut-down, no-load, dispatch). These results reveal that, at low RR levels, a switch from a deterministic to a stochastic DAM SCUC formulation results in a positive expected cost saving with respect to dispatch costs but a negative expected cost saving with respect to start-up, shut-down, and no-load costs. Conversely, at high RR levels a switch from a deterministic to a stochastic DAM SCUC formulation results in a positive expected cost saving with respect to start-up, shut-down, and no-load costs but a negative expected cost saving with respect to dispatch costs.

To understand more fully the disaggregated expected cost saving results reported in Table V, it is necessary to consider more carefully the cost trade-offs under deterministic versus stochastic DAM SCUC formulations as the RR level for deterministic SCUC increases.

Consider, first, the case in which the ISO implements a stochastic DAM SCUC optimization. By construction, the ISO will then commit enough generation in the DAM to ensure load balancing for each real-time load scenario in its anticipated load-scenario set $\mathcal{S}$, no matter how dispersed or improbable these scenarios might be. Consequently, the need to dispatch additional generation (or curtail load) in real time will tend to be reduced, assuming the ISO's anticipated load scenarios are sufficiently accurate depictions of the simulated-true load scenarios in $\mathcal{S}^T$. On the other hand, the ISO will tend to incur high UC costs because he commits sufficient generation in the DAM to balance every one of his anticipated load scenarios.

Next consider the case in which the ISO implements a deterministic DAM SCUC optimization. In this case the ISO does not consider that actual real-time loads might differ from DAM-forecasted loads (i.e., from DAM LSE demand bids). In particular, the ISO does not consider that it might be necessary to dispatch additional generation in real time to balance higher-than-forecasted loads. Consequently, once the ISO commits enough generation in the DAM to balance DAM-forecasted loads (i.e., to satisfy power balance constraints), the ISO will meet his RR constraints by committing generators in the order of their UC costs, from lowest to highest, regardless of their dispatch costs.

In particular, then, at low RR levels, implementation of the deterministic DAM SCUC results in a lower commitment of generation in comparison with the implementation of the stochastic DAM SCUC. However, implementation of the deterministic DAM SCUC incurs the risk of having to dispatch peaker units with high dispatch costs in real time, a risk that increases with increases in the dispersion of realized loads around their DAM-forecasted values. It thus incurs lower UC costs than stochastic DAM SCUC, but it also incurs higher expected dispatch costs than stochastic DAM SCUC.

Conversely, at high RR levels, implementation of the deterministic DAM SCUC results in a higher commitment of generation in comparison with the implementation of the stochastic DAM SCUC. In this case both the deterministic DAM SCUC and the stochastic DAM SCUC avoid the need to dispatch any additional generation in real time (including any

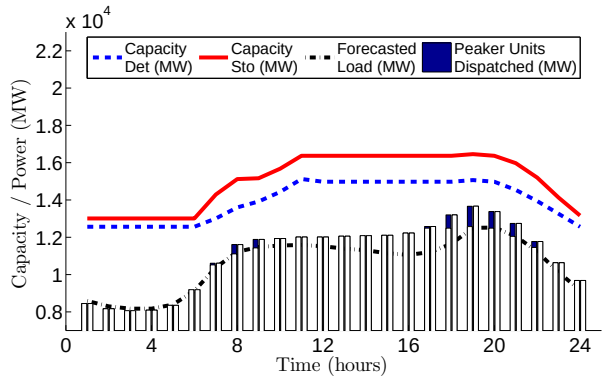

Fig. 9. Outcomes for the second day, given RR = 0% and s^* with realized load greater than forecasted load in each hour: Cost Saving = 7.33%

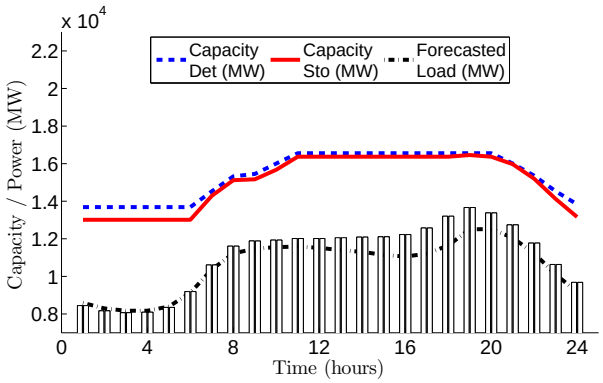

Fig. 10. Outcomes for the second day, given RR = 29% and s^* with realized load greater than forecasted load in each hour: Cost Saving = -0.07%

peaker units); but the deterministic DAM SCUC incurs higher expected UC costs due to its higher overall total committed capacity.

As the above observations suggest, the expected cost saving results reported in Table V depend strongly on the dispersion of the possible next-day loads as well as on the available mix of the generation fleet. A closer examination of specific simulation runs helps to clarify the nature of this dependence.

We first select a particular simulated-true load scenario $s^* \in \mathcal{S}^T$ for which realized (i.e., simulated-true) load is higher than the corresponding DAM-forecasted load in each hour. Three simulation runs are conducted for s^* under three different RR specifications: namely, RR=0%, RR=29%, and RR=47%. Second-day outcomes are plotted in Figs. 9, 10, and 11 for each of these three simulation runs.[12]

In Fig. 9, with RR=0%, the total committed capacity is higher under stochastic DAM SCUC since this formulation accounts for variance in loads whereas the deterministic DAM SCUC commits only enough generation to balance DAM-forecasted loads. In particular, for the deterministic DAM SCUC, the ISO bets, incorrectly, that realized (i.e., simulated true) loads will not exceed DAM-forecasted loads. The ISO is then forced to call on peaker units with very-high dispatch costs to meet higher-than-forecasted real-time loads. A switch to a stochastic DAM SCUC would result in a 7.33% cost saving for this case.

In Fig. 10, with RR increased to 29%, the total committed capacity is slightly higher under the deterministic DAM SCUC. The ISO implementing the deterministic DAM SCUC is now forced to commit more generation capacity because of the higher RR level, in comparison to the previous case with RR = 0%. However, this amount of committed generation is similar to the amount of committed generation that would

[12]In Figs. 9 through 13, the solid (red) line denotes total committed capacity under stochastic DAM SCUC, and the dashed (blue) line denotes total committed capacity under deterministic DAM SCUC. The line consisting of alternating dots and dashes denotes DAM-forecasted loads. The bars denote dispatch levels. For each hour, the left-side bar denotes the dispatch level under deterministic DAM SCUC, and the right-side bar denotes the dispatch level under stochastic DAM SCUC; these bars have equal heights because each dispatch equals realized load for that hour. Finally, blackened areas (if any) at the top of a left-side bar or right-side bar indicates a dispatch of peaker generation units under deterministic or stochastic DAM SCUC, respectively.

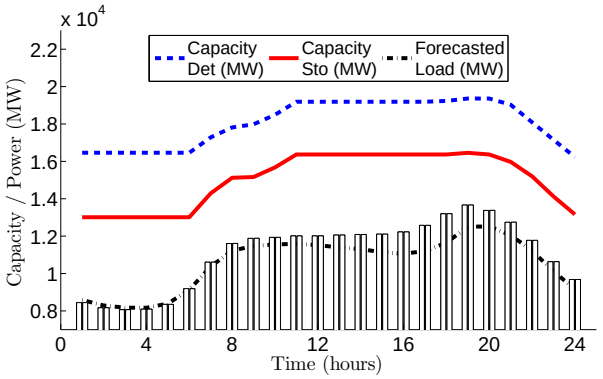

Fig. 11. Outcomes for the second day, given RR = 47% and s^* with realized load greater than forecasted load in each hour: Cost Saving = 10.03%

be committed under a stochastic DAM SCUC. Subsequently, when realized loads turn out to be higher than DAM-forecasted loads, the ISO calls on its committed generation to balance realized loads. A switch to a stochastic DAM SCUC would result in a negative cost saving of -0.07% for this case.

In Fig. 11, with RR increased all the way up to 47%, the ISO implementing a deterministic DAM SCUC has plenty of unencumbered capacity from committed generation to call on as reserve when realized loads exceed forecasted loads. However, the ISO also pays an excessive amount of UC costs for this generation. A switch to a stochastic DAM SCUC would result in a 10.03% cost saving in this case.

Now consider the selection of a particular simulated-true load scenario $s^{**} \in \mathcal{S}^T$ for which realized (i.e., simulated-true) load is *lower* than the corresponding DAM-forecasted load in each hour. Outcomes for two simulation runs conducted for s^{**} under two different RR levels, RR=0% and RR=47%, are depicted in Figs. 12 and 13, respectively.

Under either RR level, both deterministic and stochastic DAM SCUC commit enough generation capacity to meet realized loads. Under RR=0%, the stochastic DAM SCUC commits more generation capacity; hence, the stochastic DAM SCUC has higher UC costs than the deterministic DAM SCUC, and a switch from a deterministic to a stochastic DAM SCUC would result in a negative cost saving of -1.49% for this case. On the other hand, under RR=47%, it is the deterministic

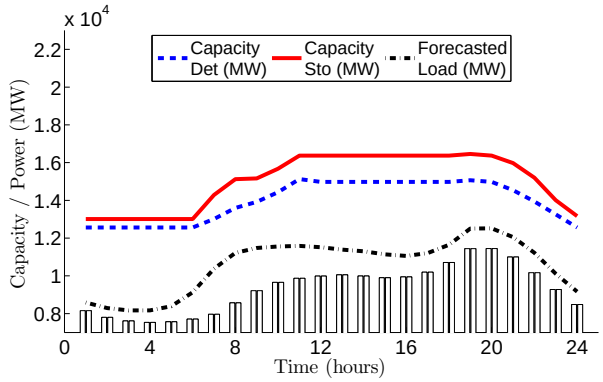

Fig. 12. Outcomes for the second day, given RR = 0% and s^{**} with realized load less than forecasted load in each hour: Cost Saving = -1.49%

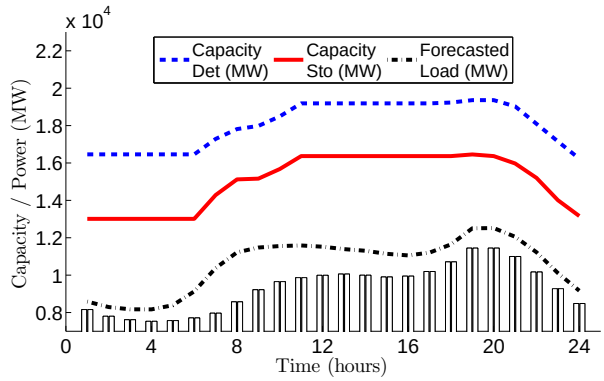

Fig. 13. Outcomes for the second day, given RR = 47% and s^{**} with realized load less than forecasted load in each hour: Cost Saving = 4.73%

DAM SCUC that commits more generation and pays more UC costs; hence, a switch from a deterministic to a stochastic DAM SCUC would result in a positive cost saving of 4.73% for this case.

VI. Concluding Remarks

To our knowledge, the 8-Zone ISO-NE Test System is the first open-source release of an empirically-grounded test system that permits the systematic study of power market design and performance issues for ISO-NE by means of systematic fast-execution computational experimentation.

For example, in Section V this test system is used to conduct comparative performance studies of alternative DAM SCUC optimization formulations for the improved handling of uncertainties when the ISO's anticipated load scenarios are biased representations of possible future load realizations. The reported findings reveal that the expected cost saving arising from a switch from a deterministic to a stochastic DAM SCUC formulation exhibits a U-shaped dependence on the reserve requirement (RR) for deterministic SCUC. The exact form of this U-shape depends in a rather complicated way on the available generation mix and on the dispersion of the possible next-day loads. Indeed, for RR levels in a neighborhood of the U-turn point, cost saving can be negative, meaning the deterministic DAM SCUC formulation outperforms the stochastic DAM SCUC formulation.

These findings demonstrate that simulation studies with small-scale test systems, such as the 8-Zone ISO-NE Test System, can help to clarify the precise conditions under which various DAM SCUC formulations are cost effective. In ongoing work we are extending this application to test the robustness of our findings to alternative specifications of the generation mix, including the addition of non-dispatchable wind power (treated as negative load) with its concomitant effects on the dispersion of net loads.

The 8-Zone ISO-NE Test System can also be used to test the effectiveness of alternative forms of reserve requirements (e.g., local versus system wide), price cap constraints, and a variety of other market design features. Another critical issue that could be explored is the extent to which market operating procedures are susceptible to manipulation for market power gain through strategic bids and offers. As noted in Section II, the test system is implemented via AMES(V4.0) [2], which permits GenCos and LSEs to be modeled as learning agents able to change their offer/bid methods over time on the basis of past experiences.

Through such exploratory studies, the 8-Zone ISO-NE Test System can facilitate understanding of current market operations. It can also function as a computational laboratory for the development of new ideas for improving these operations, and provide cautionary indications of possible adverse consequences that might result from these intended improvements.

The empirical grounding of the 8-Zone ISO-NE Test System in the structure and empirical conditions for the ISO-NE energy region could be viewed as a limitation in that it appears to narrow its range of application. Researchers wishing to apply the test system to an energy region other than ISO-NE would need to introduce a number of changes in the structural specifications and/or benchmark configurations for the test system to match the rules of operation and empirical conditions of this alternative energy region. Moreover, the test system currently models a single ISO-managed energy region, without consideration of flows with neighboring energy regions. In reality, an ISO must carefully consider power flows between its own region and neighboring energy regions.

However, as stressed throughout this study, the 8-Zone ISO-NE Test System is implemented via the modular and extensible AMES(V4.0) test bed. This should greatly ease the burden of restructuring the test system to permit the study of alternative energy regions, or to permit the study of seaming issues, if a user desires to do so.

A key limitation of the test system is its relatively small scale, which limits it to exploratory studies. The test system does not provide a test environment with suitably-high fidelity for testing the efficacy of proposed system modifications intended for immediate commercial application.

Appendix

Nomenclature

a_g	Production cost coefficient for generator g
b_g	Production cost coefficient for generator g
$B(\ell)$	Inverse of reactance (pu) on line ℓ
$C_{D,g}(k)$	Shut-down cost of g in hour k

$C_{N,g}(k)$	No-load cost of g in hour k
$C_{U,g}(k)$	Start-up cost of g in hour k
$C^s_{P,g}(k)$	Dispatch cost of g in hour k, given s
$c_{D,g}$	Shut-down cost coefficient for g
$c_{N,g}$	No-load cost coefficient for g
$c_{S,g}$	Cold-start cost coefficient for g
$E(\ell)$	End zone for line ℓ
f^{max}_ℓ	Power limit for transmission line ℓ
$\mathcal{G}$	Set of all generators g
$\mathcal{G}(z)$	Set of generators g located in zone z
$H_g(k)$	Hot-start indicator for g: 1 if hot start in hour k; 0 otherwise
$h_{S,g}$	Hot-start cost coefficient for g required to satisfy $h_{S,g} \leq c_{S,g}$
K	Set of indices k for hours of operation
$L^s(z,k)$	Zone-z load in hour k, given s
$\mathcal{L} \subset \mathcal{Z} \times \mathcal{Z}$	Set of transmission lines ℓ
$\mathcal{L}_O(z)$	Subset of lines $\ell \in \mathcal{L}$ originating at zone z
$\mathcal{L}_E(z)$	Subset of lines $\ell \in \mathcal{L}$ ending at zone z
$O(\ell)$	Originating zone for line ℓ
$p^s_g(k)$	Power output of g for hour k, given s
$\overline{p}^s_g(k)$	Maximum available power output for g in hour k, given s
$\overline{P}_g$	Maximum power output for g
$\underline{P}_g$	Minimum power output for g
$R_{D,g}$	Ramp-down limit (MW/Δk) for g
$RT_{D,g}$	$\min\{\overline{P}_g, R_{D,g}\Delta k\}$ (MW)
$R_{U,g}$	Ramp-up limit (MW/Δk) for g
$RT_{U,g}$	$\min\{\overline{P}_g, R_{U,g}\Delta k\}$ (MW)
$R_{SD,g}$	Shut-down ramp limit (MW/Δk) for g
$RT_{SD,g}$	$\min\{\overline{P}_g, R_{SD,g}\Delta k\}$ (MW)
$R_{SU,g}$	Start-up ramp limit (MW/Δk) for g
$RT_{SU,g}$	$\min\{\overline{P}_g, R_{SU,g}\Delta k\}$ (MW)
$RR(k)$	System-wide reserve requirement in hour k for deterministic DAM SCUC
S	Set of scenarios s
S_o	Positive base power (in three-phase MVA)
$T_{C,g}$	No. of cold-start hours for g
$T_{\text{off},g}$	No. of hours that g must be initially offline if $0 > \hat{v}_g(0)$; 0 if $0 < \hat{v}_g(0)$
$T_{\text{on},g}$	No. of hours that g must be initially online if $0 < \hat{v}_g(0)$; 0 if $0 > \hat{v}_g(0)$
$T_{D,g}$	Minimum down-time for g
$T_{U,g}$	Minimum up-time for g
$v_g(k)$	g's on/off status in hour k
$\hat{v}_g(0)$	g's down-time/up-time status at time 0 [13]
$w^s_\ell(k)$	Power on line ℓ in hour k, given s
$\mathcal{Z}$	Set of zones z
$\alpha^s(z,k)$	Power-balance slack term at zone z in hour k, given s
Δk	Time-period length (one hour)
$\gamma^s(z,k)$	Absolute value of $\alpha^s(z,k)$
Λ	Penalty weight for non-zero slack terms
π^s	Probability of scenario s
$\theta^s_z(k)$	Voltage angle (radians) at zone z in hour k, given s

[13] A positive (negative) value for $\hat{v}_g(0)$ indicates the number of hours prior to and including hour 0 that generator g has been turned on (off). Note that $\hat{v}_g(0)$ cannot be zero-valued.

Stochastic Unit Commitment Formulation

Objective function:

$$\sum_{k\in K}\sum_{g\in\mathcal{G}}[C_{U,g}(k)+C_{N,g}(k)+C_{D,g}(k)] + \sum_{s\in S}\pi^s\sum_{k\in K}\sum_{g\in\mathcal{G}}C^s_{P,g}(k)+\Lambda\sum_{s\in S}\pi^s\sum_{z\in\mathcal{Z}}\sum_{k\in K}\gamma^s(z,k) \quad (7)$$

ISO decision variables:

$$v_g(k),\ p^s_g(k),\ \theta^s_z(k),\quad \forall z\in\mathcal{Z}, g\in\mathcal{G}, k\in K, s\in S \quad (8)$$

ISO decision variable bound constraints:

$$v_g(k)\in\{0,1\} \qquad \forall g\in\mathcal{G}, k\in K \quad (9)$$

$$0\leq p^s_g(k)\leq\overline{P}_g \qquad \forall g\in\mathcal{G}, k\in K, s\in S \quad (10)$$

$$-\pi\leq\theta^s_z(k)\leq\pi \qquad \forall z\in\mathcal{Z}, k\in K, s\in S \quad (11)$$

Scenario-conditioned power balance constraints for each zone:

$$\sum_{g\in\mathcal{G}(z)}p^s_g(k)+\sum_{\ell\in\mathcal{L}_E(z)}w^s_\ell(k)+\alpha^s(z,k) = L^s(z,k)+\sum_{\ell\in\mathcal{L}_O(z)}w^s_\ell(k)\ ; \quad (12)$$

$$\alpha^s(z,k)=\alpha^{+,s}(z,k)-\alpha^{-,s}(z,k)\,; \quad (13)$$

$$\gamma^s(z,k)=\alpha^{+,s}(z,k)+\alpha^{-,s}(z,k) \quad (14)$$

$$\forall z\in\mathcal{Z}, k\in K, s\in S \quad (15)$$

Scenario-conditioned capacity constraints for each $g\in\mathcal{G}$:

$$\underline{P}_g v_g(k)\leq p^s_g(k)\leq\bar{p}^s_g(k), \qquad \forall k\in K, s\in S \quad (16)$$

$$0\leq\bar{p}^s_g(k)\leq\bar{P}_g v_g(k), \qquad \forall k\in K, s\in S \quad (17)$$

Scenario-conditioned limit constraints for each line $\ell\in\mathcal{L}$:

$$w^s_\ell(k)=S_o B(\ell)\left[\theta^s_{O(\ell)}(k)-\theta^s_{E(\ell)}(k)\right], \quad (18)$$

$$-f^{max}_\ell\leq w^s_\ell(k)\leq f^{max}_\ell, \qquad \forall k\in K, s\in S \quad (19)$$

Scenario-conditioned ramp constraints for each $g\in\mathcal{G}$:

$$\bar{p}^s_g(k)\leq p^s_g(k-1)+RT_{U,g}[v_g(k-1)] + RT_{SU,g}[v_g(k)-v_g(k-1)]+\bar{P}_g[1-v_g(k)], \quad \forall k\in K, s\in S \quad (20)$$

$$\bar{p}^s_g(k)\leq\bar{P}_g v_g(k+1)+RT_{SD,g}[v_g(k)-v_g(k+1)], \quad \forall k=1,\cdots,(|K|-1), \forall s\in S \quad (21)$$

$$p^s_g(k-1)-p^s_g(k)\leq RT_{D,g}v_g(k) + RT_{SD,g}[v_g(k-1)-v_g(k)] + \bar{P}_g[1-v_g(k-1)], \quad \forall k\in K, s\in S \quad (22)$$

Hot start-up constraints for each $g \in \mathcal{G}$:

$$H_g(k) = 1, \qquad 1 \le k \le T_{C,g} : (k - T_{C,g}) \le \hat{v}_g(0) \tag{23}$$

$$H_g(k) \le \sum_{t=1}^{k-1} v_g(t),\ 1 \le k \le T_{C,g} : (k - T_{C,g}) > \hat{v}_g(0) \tag{24}$$

$$H_g(k) \le \sum_{t=k-T_{C,g}}^{k-1} v_g(t), \quad \forall k = (T_{C,g}+1), \ldots, |K| \tag{25}$$

Start-up cost constraints for each $g \in \mathcal{G}$:

$$\begin{aligned} C_{U,g}(k) =& \max\{0, U_g(k)\}\,; \\ U_g(k) =& \, c_{S,g} - [c_{S,g} - h_{S,g}] H_g(k) \\ & - c_{S,g}\big[1 - [v_g(k) - v_g(k-1)]\big], \quad \forall k \in K \end{aligned} \tag{26}$$

No-load cost constraints for each $g \in \mathcal{G}$:

$$C_{N,g}(k) = c_{N,g} v_g(k),\ \forall k \in K \tag{27}$$

Shut-down cost constraints for each $g \in \mathcal{G}$:

$$\begin{aligned} C_{D,g}(k) =& \max\{0, D_g(k)\}\,; \\ D_g(k) =& \, c_{D,g}[v_g(k-1) - v_g(k)], \qquad \forall k \in K \end{aligned} \tag{28}$$

Minimum up-time constraints for each $g \in \mathcal{G}$:

$$\sum_{k=1}^{T_{\text{on},g}} [1 - v_g(k)] = 0 \text{ if } T_{\text{on},g} \ge 1\,; \tag{29}$$

$$\begin{aligned} &\sum_{n=k}^{k+T_{U,g}-1} v_g(n) \ge T_{U,g}[v_g(k) - v_g(k-1)], \\ &\forall k = (T_{\text{on},g}+1), \cdots, (|K| - T_{U,g} + 1)\,; \end{aligned} \tag{30}$$

$$\begin{aligned} &\sum_{n=k}^{|K|} (v_g(n) - [v_g(k) - v_g(k-1)]) \ge 0, \\ &\forall k = (|K| - T_{U,g} + 2), \cdots, |K| \end{aligned} \tag{31}$$

Minimum down-time constraints for each $g \in \mathcal{G}$:

$$\sum_{k=1}^{T_{\text{off},g}} v_g(k) = 0 \text{ if } T_{\text{off},g} \ge 1\,; \tag{32}$$

$$\begin{aligned} &\sum_{n=k}^{k+T_{D,g}-1} [1 - v_g(n)] \ge T_{D,g}[v_g(k-1) - v_g(k)], \\ &\forall k = (T_{\text{off},g}+1), \cdots, (|K| - T_{D,g} + 1)\,; \end{aligned} \tag{33}$$

$$\begin{aligned} &\sum_{n=k}^{|K|} \big[1 - v_g(n) - [v_g(k-1) - v_g(k)]\big] \ge 0, \\ &\forall k = (|K| - T_{D,g} + 2), \cdots, |K| \end{aligned} \tag{34}$$

Voltage angle constraints for angle reference zone 1:

$$\theta_1^s(k) = 0, \quad \forall k \in K, s \in S \tag{35}$$

ACKNOWLEDGMENT

The authors are grateful to the editor and three referees for thoughtful constructive comments. They also thank members of their DOE ARPA-E project for help with the Pyomo implementation of the stochastic SCUC formulation.

REFERENCES

[1] DOE Office of Management, "Technology Readiness Assessment Guide," Department of Energy, DOE G 413.3-4A, Tech. Rep., September 2011. [Online]. Available: https://www.directives.doe.gov/directives-documents/400-series/0413.3-EGuide-04a

[2] AMES Wholesale Power Market Test Bed Homepage. [Online]. Available: http://www.econ.iastate.edu/tesfatsi/AMESMarketHome.htm

[3] Q. Wang, J. McCalley, T. Zheng, and E. Litvinov, "A computational strategy to solve preventive risk-based security-constrained OPF," *IEEE Trans. on Power Syst.*, vol. 28, no. 2, pp. 1666–1675, May 2013.

[4] "Power System Test Case Archive," University of Washington. [Online]. Available: http://www.ee.washington.edu/research/pstca/

[5] C. Grigg and et al., "The IEEE reliability test system-1996: A report prepared by the reliability test system task force of the application of probability methods subcommittee," *IEEE Trans. on Power Syst.*, vol. 14, no. 3, pp. 1010–1020, Aug 1999.

[6] Q. Binh Dam, A. P. S. Meliopoulos, G. Heydt, and A. Bose, "A breaker-oriented, three-phase IEEE 24-substation test system," *IEEE Trans. on Power Syst.*, vol. 25, no. 1, pp. 59–67, Feb 2010.

[7] A. K. Singh and B. C. Pal, "Report on the 68-bus 16-machine 5-area system, version 3.3," IEEE PES Task Force on Benchmark Systems for Stability Controls, Tech. Rep., December 2013.

[8] R. Zimmerman, C. Murillo-Sánchez, and R. Thomas, "MATPOWER: Steady-state operations, planning and analysis tools for power systems research and education," *IEEE Trans. on Power Syst.*, vol. 26, no. 1, pp. 12–19, February 2011.

[9] J. Lally, "Financial transmission rights: Auction example," ISO New England M-06, Tech. Rep., January 2002.

[10] J. Sun and L. Tesfatsion, "Dynamic testing of wholesale power market designs: An open-source agent-based framework," *Computational Economics*, vol. 30, pp. 291–327, 2007.

[11] H. Li and L. Tesfatsion, "Development of open source software for power market research: The AMES test bed," *Journal of Energy Markets*, vol. 2, no. 2, pp. 111–128, 2009.

[12] F. Li and R. Bo, "Small test systems for power system economic studies," in *Power and Energy Society Gen. Meet., IEEE*, July 2010, pp. 1–4.

[13] FERC, "RTO unit commitment test system," Federal Energy Regulatory Commission, Tech. Rep., July 2012.

[14] J. Price and J. Goodin, "Reduced network modeling of WECC as a market design prototype," in *Power and Energy Society Gen. Meet., IEEE*, July 2011.

[15] J. Morales, A. Conejo, and J. Pérez-Ruiz, "Economic valuation of reserves in power systems with high penetration of wind power," *IEEE Trans. on Power Syst.*, vol. 24, no. 2, pp. 900–910, May 2009.

[16] A. Papavasiliou, S. Oren, and R. O'Neill, "Reserve requirements for wind power integration: A scenario-based stochastic programming framework," *IEEE Trans. on Power Syst.*, vol. 26, no. 4, pp. 2197–2206, Nov 2011.

[17] M. Vrakopoulou, K. Margellos, J. Lygeros, and G. Andersson, "A probabilistic framework for reserve scheduling and N-1 security assessment of systems with high wind power penetration," *IEEE Trans. on Power Syst.*, vol. 28, no. 4, pp. 3885–3896, Nov 2013.

[18] D. Krishnamurthy. 8-Zone ISO-NE Test System: Code and data repository. [Online]. Available: https://bitbucket.org/kdheepak89/eightbustestbedrepo

[19] FERC, "Notice of white paper," U.S. Federal Energy Regulatory Commission, April 2003.

[20] ISO-NE Homepage. [Online]. Available: http://www.iso-ne.com/

[21] A. R. Bergen and V. Vittal, *Power systems analysis*. Prentice Hall, 1999.

[22] D. Deno and L. Zaffanella, "Transmission line reference book 345 kv and above," 1982.

[23] 2013-14 ISO-NE Regional Profile. [Online]. Available: http://www.iso-ne.com/nwsiss/grid_mkts/key_facts/final_regional_profile_2014.pdf

[24] U.S. Energy Information Administration (EIA) Homepage. [Online]. Available: http://www.eia.gov/

[25] ISO New England energy offer data. [Online]. Available: http://www.iso-ne.com/isoexpress/web/reports/pricing/-/tree/day-ahead-energy-offer-data

[26] MISO Regulation Mileage Year One Analysis. [Online]. Available: https://www.misoenergy.org/Library/Repository/Tariff/FERC%20Filings/2014-02-18%20Docket%20No.%20ER12-1664-000,%20et%20al.pdf

[27] M. Carrion and J. Arroyo, "A computationally efficient mixed-integer linear formulation for the thermal unit commitment problem," *IEEE Trans. on Power Syst.*, vol. 21, no. 3, pp. 1371–1378, Aug 2006.

[28] H. Heitsch and W. Römisch, "Scenario reduction algorithms in stochastic programming," *Comp. Opt. Applic.*, vol. 24, no. 2-3, pp. 187–206, 2003.

Dheepak Krishnamurthy (S'10) received the B.E. degree in electrical and electronics engineering from the SSN College of Engineering, Anna University, Chennai, India, in 2010, and is completing an M.S. degree in the Department of Electrical and Computer Engineering at Iowa State University. He has been a design engineer for a coal-based power plant, and a research intern at Argonne National Laboratory working on storage modeling issues. Since January 2015 he has been employed at NREL in Golden, CO. His research interests include power system operations, stochastic unit commitment, and high performance computing.

Wanning Li (S'12) received the B.S. degree in electrical engineering from Harbin Institute of Technology, China, in 2011, and is completing a Ph.D. degree in the Department of Electrical and Computer Engineering at Iowa State University. She has been a research intern at MISO for the past two summers working on load forecasting, AGC enhancement with storage, and unit commitment process improvement. Her primary research area is wholesale power market design.

Leigh Tesfatsion (M'05) received the Ph.D. degree in economics from the U. of Minnesota in 1975. She is Professor of Economics, Mathematics, and Electrical and Computer Engineering at Iowa State University. Her principal research area is agent-based test bed development, with a special focus on power market design. She participates in several IEEE PES working groups and task forces focusing on power economics issues and serves as associate editor for a number of journals, including *J. of Energy Markets* and *Foundations and Trends in Energy Markets*.